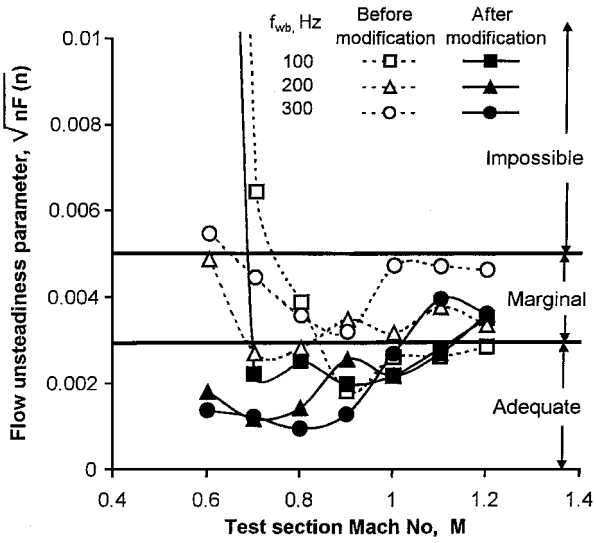

a) Criteria for light buffet onset measurements

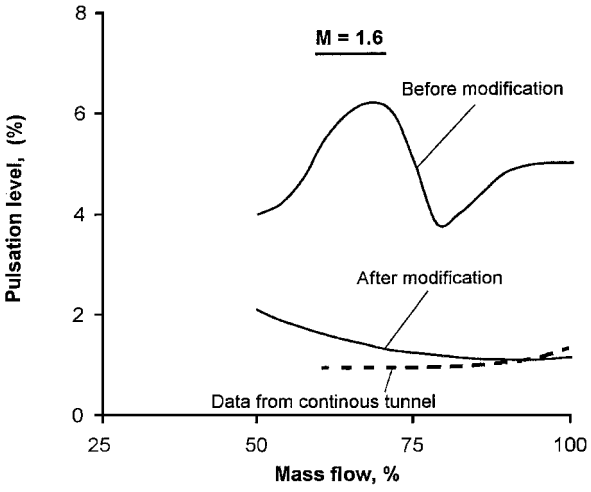

b) Comparison of pulsation measurements in air intake models

Fig. 5 Impact of improved flow quality on dynamic measurements in tunnel.

should yield more consistent and accurate data in the modified tunnel.

Figure 5(b) shows a comparison of pulsation level data (which are derived from unsteady total pressure distribution measurements across the engine face location) obtained on an aircraft intake model in the modified tunnel with data obtained on a similar model in the original tunnel, as well as a closed-circuit continuous tunnel. The pulsation levels measured in the original tunnel were 4–5 times higher than those measured in the continuous tunnel, primarily because the data were vitiated by the high levels of test-section flow unsteadiness, and the data were therefore considered erroneous. The pulsation levels measured in the modified tunnel, which are substantially lower and also close to those obtained in the continuous tunnel, are considered to reflect reality.

Conclusions

Acoustic baffles installed in the extended settling chamber of the NAL 1.2-m tunnel have substantially reduced the noise levels in its settling chamber and the SW test section. The quieter test-section flow has led to 1) a substantial improvement in the measurement accuracy of pulsation level data in air-intake models at supersonic speeds and 2) an improvement in light buffet onset measurement capability at subsonic/transonic speeds in the tunnel. However, the noise level in the PW test section is still high. Acoustic treatment of the plenum chamber aimed at mitigating the low-frequency tone observed in the PW test section is planned as a follow-on action.

References

[1]Doelling, N., "Dissipative Mufflers," *Noise Reduction*, edited by L. L. Beranek, McGraw–Hill, New York, 1960, pp. 434–451.

[2]Ohman, L. H., and Brown, D., "Performance of the New Roll-In Roll-Out Transonic Test Section of the NAE 1.5m × 1.5m Blowdown Wind Tunnel," *Proceedings of the 17th Congress of the International Council of the Aeronautical Sciences*, International Council of Aerospace Sciences and AIAA, Reston, VA, 1990, pp. 363–387.

[3]Cooksey, J. M., and Arnold, J. W., "Transonic Flow Quality Improvements in a Blowdown Wind Tunnel," *Journal of Aircraft*, Vol. 10, No. 9, 1973, pp. 554–560.

[4]Whitfield, E., "Noise and Flow Management in Blowdown Wind Tunnels," *Wind Tunnel Design and Testing Techniques*, CP174, AGARD , 1975, pp. 6-1–6-8.

[5]Dougherty, N. S., Jr., and Fisher, D. F., "Boundary-Layer Transition on a 10-Degree Cone: Wind-Tunnel/Flight-Data Correlation," AIAA Paper 800154, Jan. 1980.

[6]Ross, R., and Rohne, P. B., "Noise Environment in the NLR Transonic Wind Tunnel HST," National Aerospace Labs., Amsterdam, NLR TR 74128U, Aug. 1973.

[7]Ziegler, C. E., "Pressure Fluctuation at Supersonic Mach Numbers in the Loral Vought Systems High Speed Wind Tunnel," Loral Vought Systems, Dallas, Texas, Oct. 1984.

[8]Greening, E. S., "Modifications to the B.A.C. 4 ft H.S.T. Settling Chamber to Improve the Tunnel Flow Quality," British Aircraft Corporation, Preston, England, U.K., March 1973.

[9]Karabinus, R. J., and Sanders, B. W., "Measurements of Fluctuating Pressures in 8- by 6-Foot Supersonic Wind Tunnel for Mach Number Range of 0.56 to 2.07," NASA TM X - 2009, May 1970.

[10]Mabey, D. G., "Flow Unsteadiness and Model Vibration in Wind Tunnels at Subsonic and Transonic Speeds," Aeronautical Research Council, London, CP 1155, Oct. 1970.

Concise Orthogonal Representation of Supercritical Airfoils

G. M. Robinson*
Defence Evaluation and Research Agency, Farnborough, England GU14 6TD, United Kingdom
and
A. J. Keane†
University of Southampton, Southampton, England SO17 1BJ, United Kingdom

Introduction

THE combination of optimization algorithms and computational fluid dynamics offers promise for the development of improved aerodynamic designs. Optimization strategies have a common requirement for representation of geometry by a number of design parameters. For wing design the parameterization is generally separable into a representation of the planform and the representation of airfoil sections at a number of spanwise positions. The representation of airfoil sections is considered here with particular emphasis on the requirements of conceptual wing design.

The choice of representation depends on the type of optimization study. For two-dimensional airfoil design, representations are usually required that allow novel airfoil designs to be found. However,

Received 12 December 2000; revision received 28 January 2001; accepted for publication 7 February 2001.

*Research Fellow; currently Chief Aerodynamicist, Farnborough-Aircraft.com, Building P71, Farnborough, England, U.K.

†Professor of Computational Engineering, Director BAE Systems/Rolls-Royce University Technology Partnership for Design, School of Engineering Sciences, Highfield.

for three-dimensional wing design optimization is frequently conceptual in nature where the aim is specification of an appropriate rather than innovative airfoil for each spanwise station. The direct use of airfoil coordinates is ruled out by the number of variables required and the potential for strong coupling between the geometric specification and discretization errors. Representations that both reduce the number of design parameters and have a more global influence on geometry have therefore been sought. Closest to the direct use of coordinates is representation of all or part of the airfoil surface by B-spline or Bézier curves.[1,2] This allows innovative design at the cost of a large number of design parameters. However, as much of the resulting design space corresponds to non-airfoil-like shapes, this approach is better suited to airfoil than wing design studies. Many early wing design studies used linear combinations of existing airfoil sections,[3] the resulting shapes being "airfoil-like." Other common representations apply modifying functions such as the widely used Hicks–Henne functions[4,5] to an existing base airfoil. Concise representations without base airfoils have also been reported, for example, by superposition of Wagner functions.[6]

A disadvantage of these and many other representations proposed so far is their lack of geometric orthogonality. This implies a nonunique mapping between parameter values and geometry. The resulting spurious multimodality of the objective function degrades significantly the search process. As yet few geometrically orthogonal airfoil representations have been reported. Kuruvila et al. derived a set of four analytically defined orthogonal shape functions from the NACA four-digit airfoils, modified to have closed trailing edges.[7] Chung Chang et al. also derived the same four orthogonal functions and a further six similar functions.[8] They reported that, although only four functions are required to represent the geometry of a NACA 0012 section, the Korn supercritical airfoil requires separate representation of upper and lower surfaces, each using all 10 functions. Although these analytically derived orthogonal base functions have been applied successfully in subsonic optimization, this requirement for approximately 20 parameters limits their utility in supercritical wing design.

This Note reports the numerical derivation of a set of geometrically orthogonal base functions capable of more concise representation of supercritical sections than those derived analytically.

Derivation of Base Functions

The objective was derivation of base functions suitable for conceptual optimization of supercritical wings by selection of state of the art rather than innovative sections. The NASA SC(2) family of supercritical airfoils[9] was chosen as the starting point. Each of these airfoils was designed using a hodograph method for a particular lift coefficient and thickness-to-chord ratio; the design point being reflected in the designation [e.g., SC(2)-0612 is 12% thick with a design C_L of 0.6]. In each case the design Reynolds number was 3.0×10^6 with transition on upper and lower surfaces fixed at 3%, the design Mach number having being allowed to float during the design process.

Preliminary analyses of the SC(2) airfoils using the full potential code VGK[10] gave unexpectedly large drag values. Inspection of the coordinates suggested this resulted from the presence of large second derivatives probably arising from rounding in the tabulated coordinates. To overcome this, a Savitzk–Golay smoothing algorithm[11] was applied to the original airfoil coordinates. Drag values from full potential analyses of the smoothed airfoils were consistent with the results in NASA TP-2969.[12] Hereafter all references to SC(2) airfoils in this work refer to the smoothed airfoils, which will be given the suffix "s."

For the work described here nine airfoils (0406s, 0606s, 0706s, 0410s, 0610s, 0710s, 0412s, 0612s and 0712s) were selected as most appropriate for the mid- and outer sections of transport aircraft wings. These nine airfoils were used to derive a set of geometrically orthogonal base functions. Rather than adopting an analytical representation, each base function was characterized as a set of upper and lower z values with chordwise distribution matching the original airfoils. Each base function represented both upper and lower surfaces, the sole imposed condition being that the functions should be smooth. The first function was obtained by least-squares fitting to the smoothed airfoils and subsequent functions by fitting to the residuals from the preceding fit. Iteration was used to resolve fit nonlinearity in products of the function z values and the weighting coefficients. The requirement that the base functions be smooth was imposed by applying Savitzk–Golay smoothing to the base functions between iterations. As both numerical error and the smoothing process reduced the orthogonality of the base functions derived in this manner, Gram–Schmitt orthogonalization[11] was applied to the fitted functions to generate the final geometrically orthogonal base functions. The first five base functions are illustrated in Figs. 1 and 2.

Table 1 Geometric residuals

No. of base functions	Maximum residual	σ residual
1	7.5e−3	2.9e−3
2	3.0e−3	5.1e−4
3	1.1e−3	2.7e−4
4	5.2e−4	1.5e−4
5	3.0e−4	4.7e−5

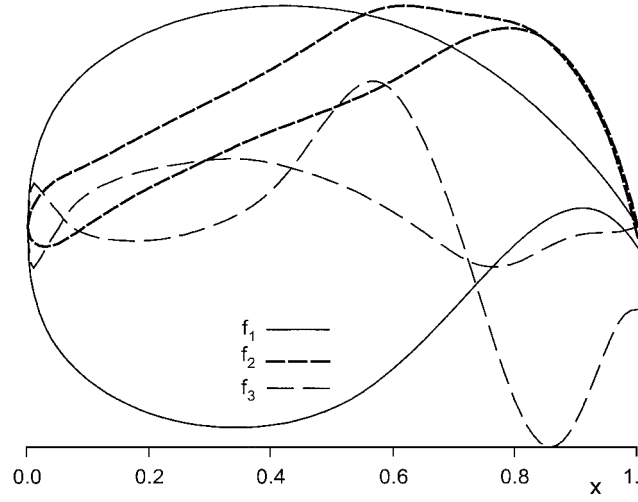

Fig. 1 First three orthogonal base functions.

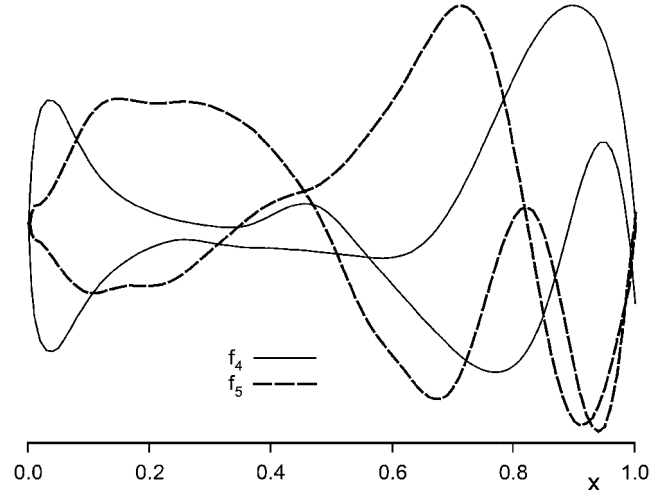

Fig. 2 Fourth and fifth orthogonal base functions.

Application

Table 1 shows the maximum values and standard deviations of the residuals from the geometric fits of different numbers of these base

functions to the nine smoothed airfoils. It is apparent that the geometry of the original airfoils can be represented adequately by use of the first four base functions only. Table 2 presents results comparing the maximum values and standard deviation of the differences in drag values between the fitted and smoothed airfoils. In each case the results were calculated using VGK with $Re = 30 \times 10^6$, $x_t = 0.03$, for design Mach numbers estimated from Ref. 12. The results indicate that only three base functions are required to fit the original smoothed airfoils so as to effectively reproduce their aerodynamic performance. Although not reported here, similar results have been obtained from orthogonalization of other more modern supercritical airfoil families.

Table 3 shows results of a further VGK study using the first two base functions only. The first function can be described as representing the mean airfoil, whereas the second function has the character of a camber adding function. In this case, rather than fitting geometrically the base functions to the airfoils, the results presented are after optimization of β (the ratio between the camber adding function and the mean airfoil), so as to minimize drag at the design point. Although the results do not infer other aerodynamic properties, they indicate that with suitable choice of β the drag performance of the original airfoils can be matched to within a few counts using airfoils constructed from only two base functions (the drags are never more than two counts worse and are sometimes significantly better). Figure 3 illustrates the section geometries resulting from this process for two of these cases (0406s and 0610s). The figure demonstrates that when the optimized airfoil has similar drag properties to those of the original section the geometric differences are slight. In the case of the 0406s airfoil where the optimized design has around 8% less drag, the differences are more marked. Investigations at design points other than those of the original airfoils suggest that low drag airfoils can be obtained throughout the design space; $0.4 < C_L < 1.0$, $0.06 < t/c < 0.12$. This suggests that for the purposes of conceptual design, supercritical airfoils could be represented by just two parameters; t/c and β. The selection of airfoils in wing conceptual design could then be reduced to optimization of the spanwise distribution of t/c and β. Optimizations of wing geometry using such an approach have been reported by the authors.[13]

Table 2 Aerodynamic drag residuals (counts)

No. of base functions	Maximum residual	σ residual
1	51.8	19.7
2	5.3	2.2
3	2.3	1.2
4	3.0	1.2
5	3.0	1.2

Table 3 Comparison of original and two base function airfoils

SC(2) airfoil	C_L	t/c	M	Drag (counts) Original	$f_1 + \beta_{\text{opt}} f_2$
0406s	0.4	0.06	0.84	74	66
0606s	0.6	0.06	0.82	74	72
0706s	0.7	0.06	0.80	70	65
0410s	0.4	0.10	0.79	72	70
0610s	0.6	0.10	0.78	83	85
0710s	0.7	0.10	0.77	87	89
0412s	0.4	0.12	0.78	84	85
0612s	0.6	0.12	0.76	90	88
0712s	0.7	0.12	0.75	90	90

Conclusion

A set of geometrically orthogonal base functions has been derived from a family of supercritical airfoils. It has been demonstrated that very few of these functions are required to approximate the aerodynamic behavior of the original airfoils. It is expected that this concise representation of these functions will be of utility in multidisciplinary optimization.

Acknowledgments

This work was funded by the U.K. Engineering and Physical Sciences Research Council under Grant GR/L04733 and also by the University Technology Partnership for Design, which is a collaboration between Rolls-Royce, BAE SYSTEMS, and the Universities of Cambridge, Sheffield, and Southampton, U.K.

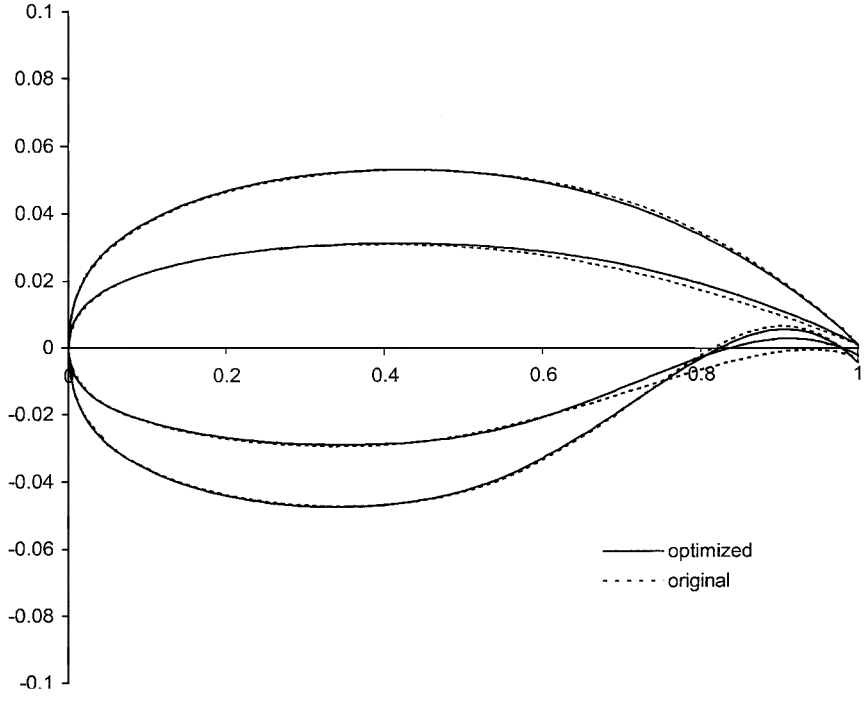

Fig. 3 Original and optimized 0406s and 0610s airfoil geometries.

References

[1]Cosentino, G. B., and Holst, T. L., "Numerical Optimization Design of Advanced Transonic Wing Configurations," NASA-TM-85950, May 1984.

[2]Jameson, A., "Aerodynamic Design via Control Theory," *Journal of Scientific Computing*, Vol. 3, 1988, pp. 233–260.

[3]Obayashi, S., and Tsukahara, T., "Comparison of Optimization Algorithms for Aerodynamic Shape Design," AIAA-96-2394-CP, AIAA, Reston, VA, 1996, pp. 181–187.

[4]Hicks, R. M., and Henne, P. A., "Wing Design by Numerical Optimization," *Journal of Aircraft*, Vol. 15, No. 7, 1978, pp. 407–412.

[5]Lores, M. E., Smith, P. R., and Large, R. A., "Numerical Optimization: An Assessment of its Role in Transport Aircraft Design Through a Case Study," *Proceedings of the 12th International Council of the Aeronautical Sciences Congress*, 1980, pp. 41–52.

[6]Onur, N., "Application of Wagner Functions in Symmetrical Airfoil Design," *Journal of Aircraft*, Vol. 34, No. 2, 1997, pp. 259, 260.

[7]Kuruvila, G., Ta'asan, S., and Salas, M. D., "Airfoil Design and Optimization by the One-Shot method," AIAA Paper 95-0478, Jan. 1995.

[8]Chang, Chung, Torres, F. J., and Tung, Chee, "Geometric Analysis of Wing Sections," NASA-TM-110346, April 1995.

[9]Harris, C. D., "NASA Supercritical Airfoils: A Matrix of Family-Related Airfoils," NASA-TP-2969, March 1990.

[10]Engineering Sciences Data Unit, "VGK Method for Two-Dimensional Airfoil Sections," ESDU-96028, London, Nov. 1996.

[11]Press, W. H., Teukolsky, S. A., Vettering, W., and Flannery, B. P., *Numerical Recipes in FORTRAN*, 2nd ed, Cambridge Univ. Press, Cambridge, England, U.K., 1992.

[12]Harris, C. D., "NASA Supercritical Airfoils—A Matrix of Family-Related Airfoils," NASA TP-2969,1990.

[13]Robinson, G. M., and Keane, A. J., "A Case for Multi-Level Optimization in Aeronautical Design," *The Aeronautical Journal*, Vol. 103, No. 1028, 1999, pp. 481–485.

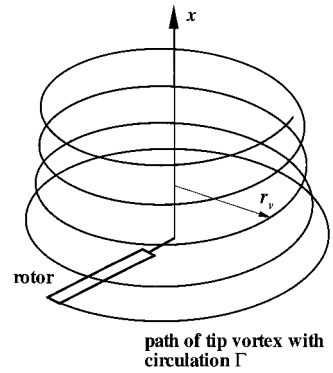

Fig. 1 Geometry of the tip vortex of a single-bladed rotor; angular velocity of the blade is Ω rad/s.

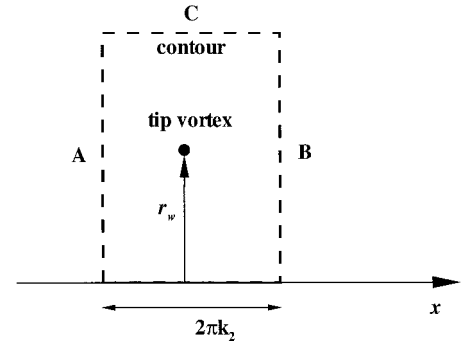

Fig. 2 Rectangular circuit used to derive Eq. (1).

Effect of Tip Vortex Geometry on the Flow Through the Blades of Hovering Rotors

D. H. Wood*

University of Newcastle, Callaghan, New South Wales 2308, Australia

Introduction

IT is well known that the average velocity through the blades of a hovering rotor, U_b, is greater than half the average velocity in the far wake, U_w, the value required by simple momentum theory. This is reflected in the ratio of the radius of the far wake, r_w, to the blade tip radius r_b, which has an experimental value of around 0.78, rather than $2^{-1/2}$ (e.g., see Leishman[1]). The purpose of this Note is to investigate the role of wake geometry, in the form of the pitch and radius of the tip vortices, in producing the discrepancy. It is suggested that the discrepancy is due mainly to the change in pitch of the tip vortices and is reduced by their contraction. The basic geometry of the rotor and the tip vortex is shown Fig. 1 for a single-blade rotor.

Formulation and Analytical Results

It is necessary to establish the following relation between the circulation of each tip vortex, Γ, and U_w:

$$U_w = N\Gamma/(2\pi k_2) \tag{1}$$

where N is the number of blades and k_2 is the pitch of the tip vortices in the far wake. To do this, consider the circulation around the rectangular circuit shown in Fig. 2 with one of the two legs of length $2\pi k_2$ placed along the axis of rotation ($r = 0$). The radial legs (A and B in Fig. 2) are greater than r_w, to enable the circuit to enclose N tip vortices without cutting them. Thus, the area integral of vorticity within the circuit is $N\Gamma$. Because the contribution to the circulation around the circuit from the two radial legs will cancel and that of the outer leg C will be zero, Eq. (1) gives the velocity along the axis of rotation. If the radial leg of the contour is now reduced to be less than r_w, then the circulation becomes zero, which requires Eq. (1) to be independent of radius in the far wake.

Relation (1) is strictly valid only if all of the tip vorticity is confined within tip vortices of constant pitch and radius and the hub vorticity is confined to N straight vortex lines lying along the axis of rotation. This is a simplification of the structure of real wakes and may well be the reason for the overestimated value for Γ that can be determined from Eq. (1) as follows. The single rotor data of Leishman et al.[2] indicate that the velocity in the wake is reasonably uniform with r. When normalized by r_b and Ω, the angular velocity of the blades, the velocity was 0.073 at the last measuring position, $x/r_b = 0.399$ (see their Fig. 7), where the wake had not fully contracted. Their formula (2) for the development of the tip vortex radius allows U_w to be estimated as 0.0783. Using $k_2 = 0.041$ from their Table 2 gives $\Gamma/\Omega r_b^2 = 0.020$, which compares with the measured values in the range of 0.010–0.015 from their Fig. 13. Nevertheless, the simplicity of Eq. (1) allows the qualitative assessment of the effects of the tip vortex geometry.

To a similar level of simplification as that underlying Eq. (1), U_b is determined solely by the tip vortices. If the Biot–Savart law is written for $r = 0$ and the variation of U_b with r is ignored, then

$$U_b = \frac{N\Gamma}{4\pi}\int_0^\infty \frac{r_v^2}{k\left(r_v^2 + x^2\right)^{\frac{3}{2}}}\,\mathrm{d}x \tag{2}$$

where r_v and k are the radius and pitch, respectively, of the tip vortices. The former is shown in Fig. 1 along with the coordinate x, which originates at the blades. Evaluating the Biot–Savart law

Received 15 November 2000; revision received 20 December 2000; accepted for publication 7 January 2001.

*Associate Professor, Department of Mechanical Engineering.